Comparison of global sectoral methane emissions inferred by high-resolution inversion of observations from GOSAT and GOSAT-2 during 2019-2020.

Rajesh Janardanan[1], Shamil Maksyutov[1], Fenjuan Wang[1], Lorna Nayagam[1], Marielle Saunois[2], Xin Lan[3,4], Tsuneo Matsunaga[1]

1. National Institute for Environmental Studies, Japan
2. Laboratoire des Sciences du Climat et de l'Environnement, Paris, France
3. Cooperative Institute for Research in Environmental Sciences, University of Colorado Boulder, Boulder, CO, United States of America
4. NOAA Global Monitoring Laboratory, Boulder, CO, United States of America

Background

- Atmospheric abundance of methane growing faster especially in the recent decade.
- Country-wise sectoral emission estimates are important in coordinating reduction measures, so is the contribution from each sectors within a country.
- We used methane observations from global surface observation networks and GOSAT and GOSAT-2 satellites in a high-resolution methane inverse model to infer surface anthropogenic fluxes over major emitting countries.
- The objective is to check the consistency of inversions using observations from the two satellites, which is important to continue estimating emissions in the coming years with the observations from the new instrument.

Data used in the model

- **Prior fluxes**

Anthropogenic (- oil & gas)	• EDGAR v6 (Crippa et al., 2020)
Oil & gas	• GAINS (Höglund-Isaksson, 2012)
Biomass burning	• GFED v4 (Randerson et al., 2017)
Wetlands, termites	• Saunois et al. (2020).
Ocean	• Weber et al. (2019)
Geological	• Etiope et al. (2019)
Soil sink	• Murguia-Flores et al. (2018)

- **Observations**
  GOSAT NIES L2 v02.95, GOSAT-2 NIES L2 v02.00
  GLOBALVIEWplus_v4.0_2021-10-14, (Schuldt et al., 2021)
  The ICOS network (ICOS RI, 2021).
- **Meteorology**
  From ERA5 (Hersbach et al., 2020) and JRA55 (Kobayashi et al., 2015)

Inverse modeling system

- NTFVAR, coupled Eulerian-Lagrangian transport model (NIES-TM resolution 2.5°×2.5° + FLEXPART model resolution 0.1°×0.1°) (Maksyutov et al., 2021)
- Inversion period: 2009 – 2020
- National Institute for Environmental Studies (NIES) model and FLEXPART as the Lagrangian particle dispersion model.
- The model development were reported by Maksyutov et al. (2021) and application to methane inversion reported in Wang et al., (2019) and Janardanan et al., (2020).
- Model makes flux adjustments for the natural (wetland), and biomass burning, agriculture, waste, oil and gas and coal sectors of the anthropogenic emissions.
- Analysis for sectoral emissions are carried out on grid (1º×1º) and country totals.
- The model uncertainty were estimated, based on ensemble of inversions with randomly perturbed prior and observations (Chevallier et al., 2007).

Results

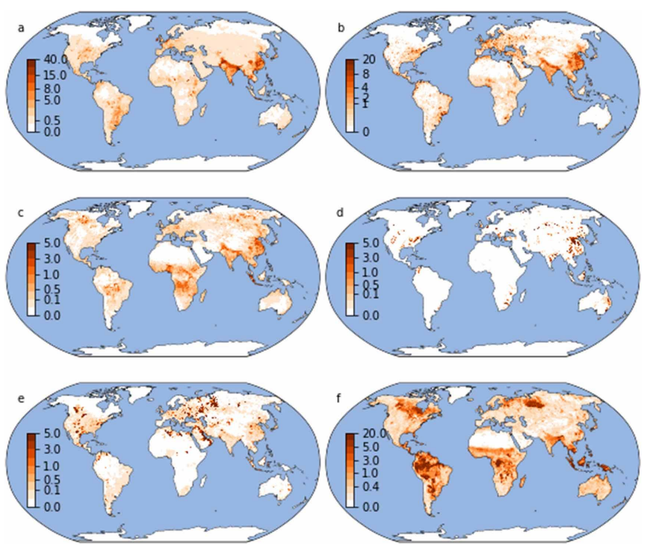

Figure 1. Mean (2019–2020) prior sectoral methane fluxes used in this study (gCH_4 m^{-2} yr^{-1}) for (a) agriculture, (b) waste, (c) biomass burning, (d) coal, (e) oil and gas, and (f) wetlands sectors.

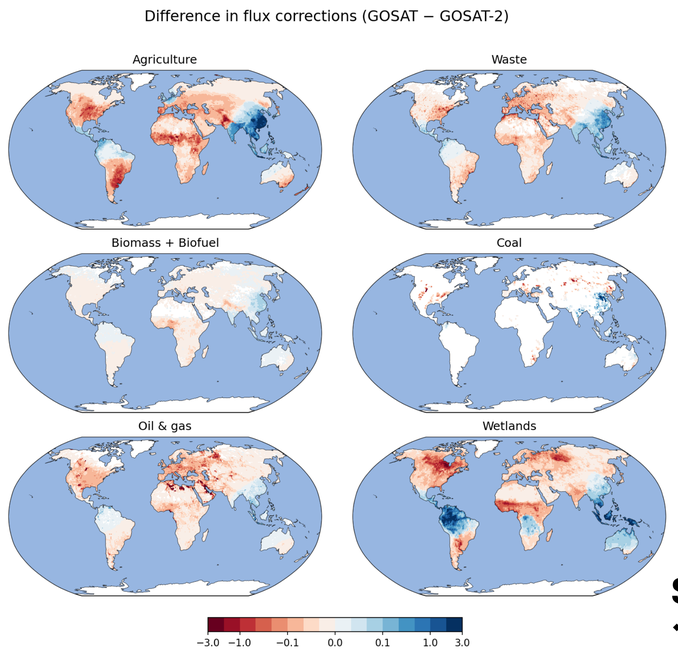

Figure 3 Mean (2019–2020) difference in sectoral methane flux corrections on a 1x1 ° (gCH_4 m^{-2} yr^{-1}) for agriculture, waste, biomass and biofuel burning, coal, oil and gas, and wetlands sectors

❖ **Agriculture**

The largest difference between the two sets of inversion globally is for the Agriculture sector. GOSAT-2 estimates lower emissions over southeastern Asia and South American tropical regions and higher emissions over south American temperate, northern tropical Africa, Eastern US and rest of Asia (Figure 3)

❖ **Waste**

GOSAT-2 estimates lower emissions over eastern China and India and higher emissions over Europe and Northeastern United states

❖ **Biomass & biofuel burning**

GOSAT and GOSAT-2 estimates similar fluxes for biomass and biofuel burning with slightly lower estimate by GOSAT-2 over eastern China and slightly higher values over Gangetic plain and tropical Africa.

❖ **Coal**

GOSAT-2 suggests higher emissions from Coal production over pockets of Russia, Europe and United States and lower emissions from China, India and Indonesia.

❖ **Oil & gas**

The largest difference between GOSAT and GOSAT-2 for Oil & gas sector is for northern Africa (Algeria, Libya), parts of Europe and southwest regions of Asia (Saudi Arabia, Iran), largest sources in the United States like the Permian Basin and regions of Russia. GOSAT-2 suggests higher emissions from these regions, whereas in northern tropical South America and southeastern regions of Asia (e.g. Indonesia) GOSAT-2 estimated lower emissions than GOSAT.

❖ **Wetlands**

GOSAT-2 reduced the exceptional upward correction in Janardanan et al 2020, 2024 in South American tropical region to a reasonably even correction. Similarly, over southeastern Asia and to a lesser degree in African regions around and south of Congo, GOSAT-2 suggests lower wetland emissions than GOSAT. The Congo basin was reported to be a major source of the 2020 surge in methane emissions (e.g. Qu et al, 2022, Janardanan et al 2024)

The country-total sectoral emissions and their uncertainties are given in Table 1

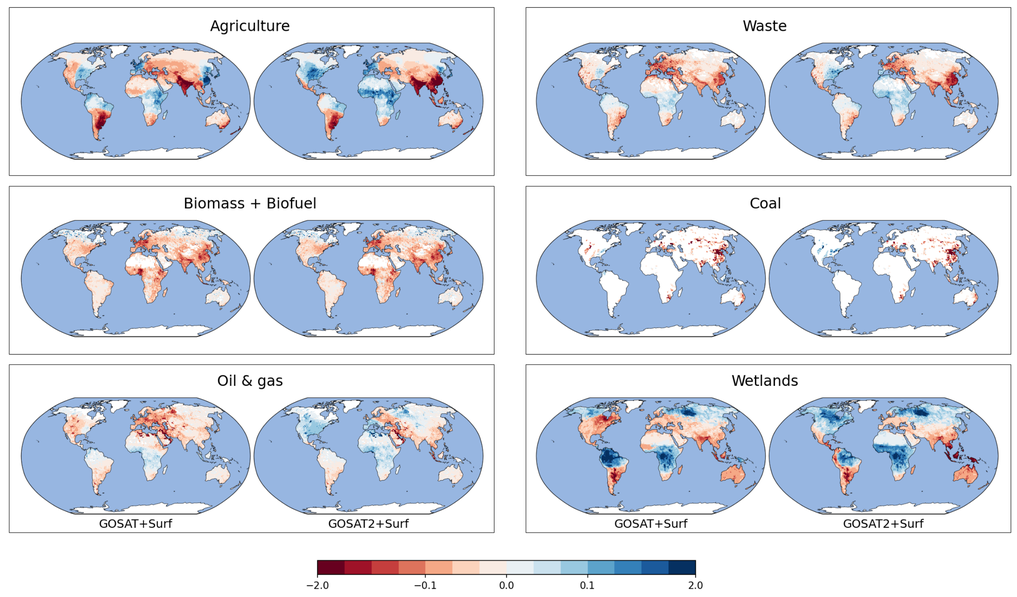

Figure 2. Mean (2019–2020) sectoral methane flux corrections (gCH_4 m^{-2} yr^{-1}) for (a) agriculture, (b) waste, (c) biomass burning, (d) coal, (e) oil and gas, and (f) wetlands sectors. Left panel of each set shows GOSAT and right GOSAT-2

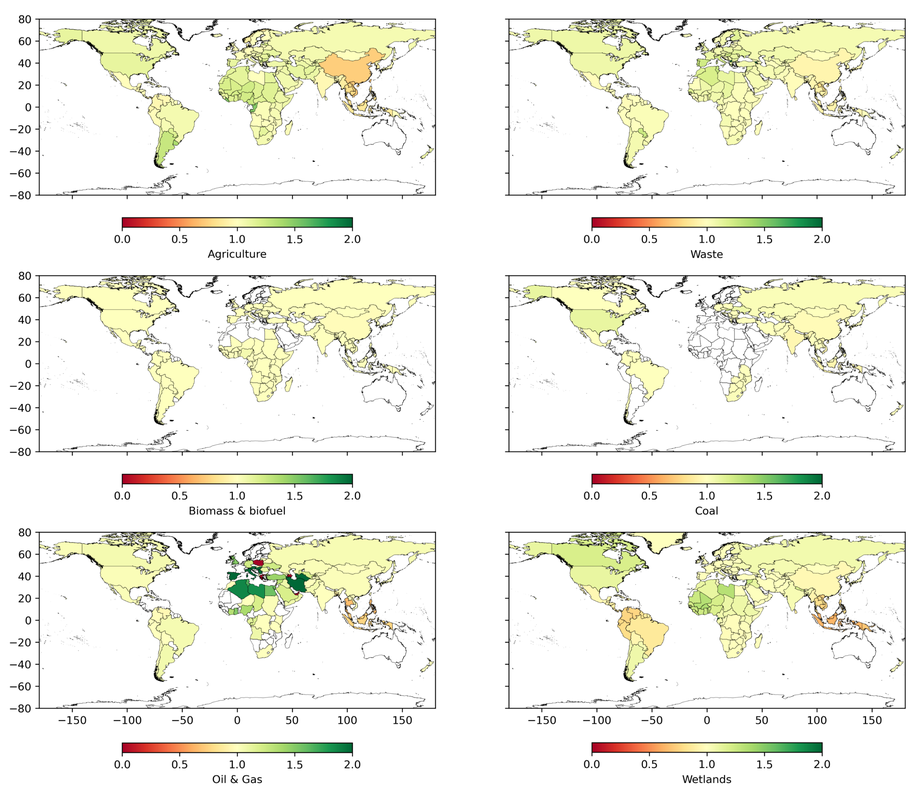

Figure 3 Ratio of GOSAT-2 to GOSAT mean (2019–2020) sectoral posterior emission country totals for agriculture, waste, biomass and biofuel burning, coal, oil and gas, and wetlands sectors

Sectors	Agriculture		Waste		Biomass and biofuel		Coal		Oil&Gas		Wetland	
Country	GOSAT	GOSAT2	GOSAT	GOSAT-2	GOSAT	GOSAT-2	GOSAT	GOSAT-2	GOSAT	GOSAT-2	GOSAT	GOSAT-2
ARG	2.34±0.25	2.97±0.31	0.52±0.01	0.55±0.01	0.11±0.00	0.11±0.00	0.00±0.00	0.00±0.00	0.44±0.01	0.47±0.01	3.58±0.15	3.86±0.16
AUS	1.89±0.24	2.04±0.26	0.31±0.01	0.31±0.01	0.88±0.02	0.88±0.02	0.79±0.05	0.79±0.05	0.27±0.00	0.26±0.00	3.84±0.16	3.40±0.14
BOL	0.72±0.02	0.75±0.02	0.08±0.00	0.08±0.00	0.44±0.00	0.44±0.00	0.00±0.00	0.00±0.00	0.12±0.00	0.12±0.00	4.68±0.27	4.38±0.26
BRA	13.52±0.36	14.29±0.38	4.91±0.09	5.06±0.09	1.85±0.04	1.85±0.04	0.05±0.00	0.05±0.00	0.22±0.01	0.23±0.01	30.50±1.67	26.19±1.44
CAN	1.06±0.02	1.15±0.02	0.57±0.01	0.62±0.01	0.46±0.00	0.46±0.00	0.08±0.01	0.08±0.01	2.68±0.11	2.84±0.12	11.20±0.70	13.49±0.84
CHN	23.18±1.54	16.82±1.12	14.36±0.70	13.35±0.65	2.47±0.03	2.42±0.03	18.97±0.98	18.31±0.95	2.69±0.02	2.75±0.02	3.03±0.09	2.92±0.09
COL	1.89±0.05	1.80±0.05	0.82±0.01	0.80±0.01	0.07±0.00	0.07±0.00	0.20±0.00	0.20±0.00	0.44±0.02	0.43±0.02	6.19±0.35	4.71±0.27
COG	0.02±0.00	0.03±0.00	0.03±0.00	0.03±0.00	0.08±0.00	0.08±0.00	0.00±0.00	0.00±0.00	0.06±0.00	0.07±0.00	5.97±0.25	5.95±0.25
COD	0.30±0.00	0.31±0.00	0.64±0.02	0.64±0.02	1.35±0.04	1.35±0.04	0.00±0.00	0.00±0.00	0.02±0.00	0.02±0.00	13.59±0.80	13.44±0.79
IND	16.37±1.63	15.73±1.56	6.56±0.15	6.44±0.15	1.23±0.05	1.23±0.05	1.11±0.05	1.05±0.05	0.47±0.01	0.47±0.01	3.92±0.17	4.06±0.17
IDN	3.70±0.34	3.20±0.30	2.04±0.11	1.89±0.10	2.17±0.01	2.17±0.01	4.83±0.30	4.53±0.28	0.79±0.06	0.60±0.04	12.12±0.77	7.72±0.49
IRQ	0.13±0.02	0.14±0.03	0.44±0.01	0.46±0.01	0.00±0.00	0.00±0.00	0.00±0.00	0.00±0.00	6.38±0.96	6.91±1.04	0.09±0.00	0.10±0.00
MEX	2.67±0.05	2.65±0.05	2.48±0.03	2.43±0.03	0.21±0.00	0.21±0.00	0.01±0.01	0.01±0.01	0.29±0.02	0.30±0.02	1.35±0.05	1.29±0.05
NGA	1.85±0.04	2.25±0.05	1.47±0.02	1.57±0.02	0.85±0.01	0.90±0.01	0.00±0.00	0.00±0.00	2.08±0.37	2.86±0.51	1.77±0.11	2.09±0.13
PAK	5.34±0.37	5.87±0.41	1.30±0.03	1.33±0.04	0.32±0.01	0.33±0.01	0.03±0.00	0.03±0.00	0.53±0.03	0.56±0.04	0.16±0.01	0.16±0.01
PER	0.53±0.00	0.52±0.00	0.27±0.00	0.27±0.00	0.04±0.00	0.04±0.00	0.00±0.00	0.00±0.00	0.03±0.00	0.03±0.00	7.80±0.53	6.18±0.42
RUS	1.59±0.02	1.67±0.02	3.36±0.03	3.53±0.04	2.93±0.35	2.93±0.35	3.15±0.13	3.24±0.13	15.78±0.41	16.36±0.43	14.54±1.19	15.50±1.27
SDN	2.58±0.03	2.98±0.04	0.44±0.01	0.45±0.01	0.34±0.00	0.34±0.00	0.00±-0.00	0.00±-0.00	0.59±0.02	0.61±0.02	3.13±0.23	3.40±0.25
THA	2.50±0.49	2.01±0.39	0.95±0.03	0.87±0.03	0.13±0.03	0.13±0.03	0.01±0.00	0.01±0.00	0.12±0.01	0.08±0.01	1.10±0.08	0.89±0.06
USA	9.63±0.29	10.79±0.32	4.29±0.05	4.62±0.06	0.68±0.08	0.68±0.08	1.44±0.28	1.60±0.31	20.57±0.28	21.09±0.29	5.58±0.28	6.20±0.32
VEN	1.17±0.02	1.12±0.02	0.36±0.00	0.36±0.00	0.15±0.01	0.15±0.01	0.01±0.00	0.01±0.00	0.47±0.01	0.45±0.01	4.52±0.35	3.44±0.26

Table 1. Country total sectoral emissions estimated by the inverse model using GOSAT and GOSAT-2 observations

Summary

❖We inverted methane observations from GOSAT and GOSAT-2 satellites together with data from surface networks to compare the posterior sectoral fluxes for the years 2019-2020

❖The strongest contrast between the two inversions was for Agriculture, Waste and Wetland emissions followed by oil & gas and Coal sectors.

❖Significant difference for wetland emissions were found for regions with large cloud cover, such as the monsoon Asia and the tropical South America. A possible reason could potentially be the larger volume of useful observations from GOSAT-2 over these regions.

❖In all sectors, GOSAT-2 tend to estimate lower emissions over southeaster Asian region. The reasons behind this need to be investigated.

References

- Maksyutov S *et al* 2021 Technical note: a high-resolution inverse modelling technique for estimating surface CO_2 fluxes based on the NIES-TM-FLEXPART coupled transport model and its adjoint *Atmos. Chem. Phys.* **21** 1245–66
- Murguia-Flores F, Arndt S, Ganesan A L, Murray-Tortarolo G and Hornibrook E R C 2018 Soil Methanotrophy Model (MeMo v1.0): a process-based model to quantify global uptake of atmospheric methane by soil *Geosci. Model. Dev.* **11** 2009–32
- Etiope G, Ciotoli G, Schwietzke S and Schoell M 2019 Gridded maps of geological methane emissions and their isotopic signature *Earth Syst. Sci. Data* **11** 1–22
- ICOS RI 2021 ICOS atmosphere release 2021-1 of level 2 greenhouse gas mole fractions of CO_2,CH_4,N_2O, CO, meteorology and 14CO2
- Kobayashi S, Ota Y, Harada Y, Ebita A, Moriya M, Onoda H and Takahashi K 2015 The JRA-55 reanalysis: general specifications and basic characteristics *J. Meteorol. Soc. Jpn.* **93** 5–48
- Kuze A, Suto H, Nakajima M and Hamazaki T 2009 Thermal and near infrared sensor for carbon observation Fourier-transform spectrometer on the greenhouse gases observing satellite for greenhouse gases monitoring *Appl. Opt.* **48** 6716
- Höglund-Isaksson L 2012 Global anthropogenic methane emissions 2005–2030: technical mitigation potentials and costs *Atmos. Chem. Phys.* **12** 9079–96
- Saunois M *et al* 2020 The global methane budget 2000–2017 *Earth Syst. Sci. Data* **12** 1561–623
- Yokota T, Yoshida Y, Eguchi N, Ota Y, Tanaka T, Watanabe H and Maksyutov S 2009 Global concentrations of CO_2 and CH_4 retrieved from GOSAT: first preliminary results *Sola* **5** 160–3
- Yoshida Y N *et al* 2013 Improvement of the retrieval algorithm for GOSAT SWIR XCO_2 and XCH_4 and their validation using TCCON data *Atmos. Meas. Tech.* **6** 1533–47
- Janardanan *et al*, Country-level methane emissions and their sectoral trends during 2009–2020 estimated by high-resolution inversion of GOSAT and surface observations 2024 *Environ. Res. Lett.* **19** 034007**DOI** 10.1088/1748-9326/ad2436
- Janardanan, R.; Maksyutov, S.; Tsuruta, A.; Wang, F.; Tiwari, Y.K.; Valsala, V.; Ito, A.; Yoshida, Y.; Kaiser, J.W.; Janssens-Maenhout, G.; et al. Country-Scale Analysis of Methane Emissions with a High-Resolution Inverse Model Using GOSAT and Surface Observations. *Remote Sens.* **2020**, *12*, 375. https://doi.org/10.3390/rs12030375
- Qu Z, Jacob D J, Zhang Y, Shen L, Varon D J, Lu X, Scarpelli T, Bloom A, Worden J and Parker R J 2022 Attribution of the 2020 surge in atmospheric methane by inverse analysis of GOSAT observations *Environ. Res. Lett.* **17** 094003
- Lan, X., E.J. Dlugokencky, J.W. Mund, A.M. Crotwell, M.J. Crotwell, E. Moglia, M. Madronich, D. Neff and K.W. Thoning. (2022), Atmospheric Methane Dry Air Mole Fractions from the NOAA GML Carbon Cycle Cooperative Global Air Sampling Network, 1983-2021, Version: 2022-11-21, https://doi.org/10.15138/VNCZ-M766